Matrix Fabry–Perot resonance mechanism in high-contrast gratings

Vadim Karagodsky, Christopher Chase, and Connie J. Chang-Hasnain*

Department of Electrical Engineering and Computer Sciences, University of California, Berkeley, California 94720, USA
**Corresponding author: cch@eecs.berkeley.edu*

Received February 22, 2011; accepted March 17, 2011;
posted April 1, 2011 (Doc. ID 142444); published April 29, 2011

We present a simple analytic formalism to explain the unique resonance phenomenon in subwavelength high-contrast gratings (HCG). We show that the resonances are due to strong coupling between two surface-normal waveguide array modes resulting from abrupt and large index contrast. Simple expression for HCG quality factor is derived that agrees with spectral-fitting approaches reported in literature. © 2011 Optical Society of America

OCIS codes: 050.2770, 050.6624, 230.5750.

Optical gratings are well understood in the context of interference of distributed reflections. A vast range of applications utilizes their properties to provide spectrally resolved diffraction or coupling. Specifically, dielectric gratings with subwavelength periods have excited much attention [1–4] due to their high optical coupling efficiency with the elimination of high diffraction orders. We recently pointed out that rather extraordinary characteristics can be achieved with a subwavelength grating that is completely surrounded by low-index media, which is hence named high-contrast grating (HCG) [5]. We discovered that HCG could be designed to have an extremely large bandwidth of high reflection [6]. We experimentally incorporated HCG in vertical cavity surface emitting lasers (VCSELs), replacing conventional distributed Bragg reflector (DBR) mirrors [7], and as a means to increase tuning speed in a tunable VCSEL [8] and to provide polarization control [5].

Most interestingly, HCG can be also designed to behave as an *optical resonator* with an ultrahigh quality factor (Q) that facilitates surface-normal output coupling [9]. The applications of HCG resonators (HCG-R) are very broad. One possibility is to embed an active region inside the grating bars, and create a surface emitting laser based solely on a single grating—a structure far simpler than a conventional VCSEL. Another possibility is to use such resonant gratings as biosensors [9]. This rather surprising and unexplored resonance phenomenon in HCGs was also experimentally demonstrated [9]. However, in that case, a rather complex structure was used, which included DBRs at the bottom and along the sides of the HCG-R. In this Letter, we show that a high Q can be obtained with a single HCG without DBRs. More importantly, we provide for the first time a *simple*, intuitive yet rigorous and analytic explanation of HCG resonance phenomenon. We show that the HCG resonance mechanism can be understood in terms of a "matrix" Fabry–Perot (FP) resonance and present a novel formulation for the HCG Q factor based on a simple generalization of a standard FP resonance case. The numerous advantages of HCGs over ordinary FP cavities are also discussed in this Letter. Other rigorous electromagnetic treatments of gratings and similar periodic structures exist in literature [10–12]. However, most of them tend to have a highly complex mathematical nature. Our emphasis in this Letter is therefore on combining rigor with simplicity without compromise in either.

An HCG is schematically shown in Fig. 1(a). For simplicity in analysis, the grating is assumed to be infinite in the y direction and infinitely periodic in the x direction. The grating has a thickness of t_g, and $z = -t_g$ and $z = 0$ are referred to as the input and output planes, respectively. The grating bars are made of a passive dielectric material with refractive index n_r. The grating bar width, period, and duty cycle are s, Λ, and $\eta = s/\Lambda$, respectively. Because of the lateral periodicity (x direction), the HCG supports multiple (waveguide array) modes propagating in the z direction whose analytical formula can be found in [13,14]. In a typical HCG with a large index contrast ($n_r \sim 2.7$–3.6), only the first two HCG modes have real propagation constants and are propagating in z direction over a relatively large spectral range, whereas the higher-order modes have imaginary propagation constants (along z), corresponding to decaying (surface) waves. The propagation (or decay) of the modes along the z axis is described by the propagation constants β_m, m being the mode number [14].

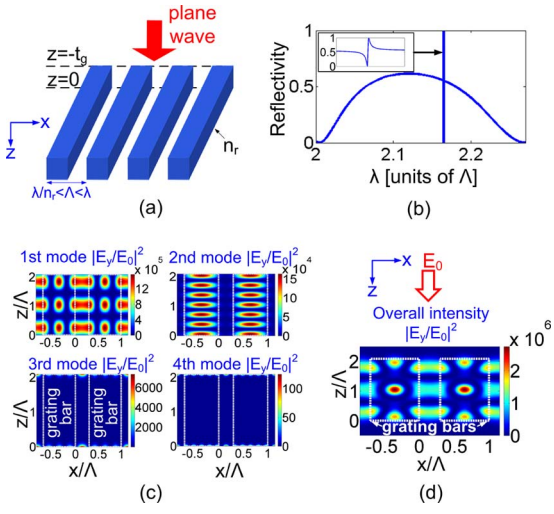

Fig. 1. (Color online) (a) High-contrast grating (HCG) resonator schematic. Λ denotes grating period. (b) Surface-normal reflectivity spectrum of HCG resonator, where the resonance is manifested by a very sharp transition between 0% and 100% reflectivity values. (c) Contour plot of the first four HCG grating modes that sum up to the overall resonator supermode in (d).

The HCG resonance phenomenon is analyzed as follows. An incident plane wave excites a superposition of HCG modes with coefficients described by a vector $\mathbf{C} = (C_1, C_2 \ldots)^T$, where C_m is the weight of mth mode at the input plane ($z = -t_g$). While propagating downward to the output plane ($z = 0$), the weight vector becomes $\varphi\mathbf{C}$, whereby φ is a diagonal propagation matrix [14], given by $\varphi_{\mathrm{mm}} = \exp(-j\beta_m t_g)$. The modes are then reflected from the output plane ($z = 0$) back up into the grating (i.e., along $-z$ direction). Upon reflection, the weight vector becomes $\boldsymbol{\rho}\varphi\mathbf{C}$, where $\boldsymbol{\rho}$ is the reflection matrix, describing the reflection of each mode into itself as well as coupling into others [14]. After one full round trip (from $z = -t_g$ to $z = 0$ and back to $z = -t_g$) the weight vector evolves into $\boldsymbol{\rho}\varphi\boldsymbol{\rho}\varphi\mathbf{C}$.

The HCG resonance occurs when the assembly of modes, $\mathbf{C}$, is *self-sustainable*. We will use the term "supermode" below for such assembly of modes. This can be compactly written as: $\mathbf{C} = \boldsymbol{\rho}\varphi\boldsymbol{\rho}\varphi\mathbf{C}$, meaning that after one round trip, the assembly of modes constructively interferes with itself, or equivalently: $(\mathbf{I} - \boldsymbol{\rho}\varphi\boldsymbol{\rho}\varphi)\mathbf{C} = \mathbf{0}$, $\mathbf{I}$ being a unit matrix. Clearly, for a nonzero solution to exist to such equation, the following condition must be satisfied:

$$\det[\mathbf{I} - (\boldsymbol{\rho}\varphi)^2] = 0. \tag{1}$$

Equation (1) is the HCG resonance condition. Furthermore, it is a multimode paraphrase on the theory of regular (single-mode) FP resonances. It is most interesting to note that in HCG-R, it is the entire supermode that is self-sustainable, while the individual modes may or may not resonate. This is why matrix representation is required and is particularly applicable.

The HCG resonance manifests itself as a sharp change in its surface-normal reflectivity spectrum, as depicted by Fig. 1(b), where reflectivity is changed from 0 to 100% over a very small wavelength range ($\Delta\lambda \sim \lambda/Q \sim 10\,\mathrm{fm}$). These transients typically ride on a background reflectivity with certain undulation. The simulation method used here is rigorous coupled wave analysis (RCWA) [15] with $\eta = 0.7$, $t_g = 2.086\Lambda$, and $n_r = 3.48$ (typical of Si at $\lambda \sim 1.55\,\mu\mathrm{m}$). In this case, polarization of incidence is parallel to the grating in y direction, known as TE polarization.

Figure 1(c) shows the intensity contour plots of the first four modes at resonant wavelength, $\lambda = 2.164\Lambda$. Figure 1(d) shows the overall field intensity inside HCG-R, which corresponds to a supermode comprising of all grating modes combined. The intensities in Figs. 1(c) and 1(d) are calculated using the method described in [14], and they are normalized by the E-field intensity of the incident plane wave ($|E_0|^2$). The overall intensity is shown to be more than two million times stronger than the intensity of the incident plane-wave—a consequence of high-Q resonant energy buildup. It is important to note that the convergence of mode strengths is very fast: the first two modes contain more than 99.7% of the overall intensity. Figure 1(c) also demonstrates that the first two HCG modes have a standing wave profile in z direction, while the third and the fourth modes are surface waves, i.e., existing only close to the HCG input and output surfaces. The HCG-R supermode shown in Fig. 1(d) is a third-order resonance, since the overall intensity exhibits three peaks along the z axis. In fact, HCG resonances can exhibit all possible orders, depending on the wavelength and the grating dimensions.

The remarkable differences between HCGs and ordinary FP resonators follow. In the case of a regular FP cavity with length t, the resonant condition is the scalar version of Eq. (1): $[\rho\exp(-j\beta t)]^2 = 1$, ρ being a reflection coefficient from the FP wall and β being the propagation wavenumber. This condition can be satisfied either with *gain medium*, $\mathrm{Im}(\beta) > 0$, $|\rho| < 1$, or with *highly reflecting walls*, $|\rho| = 1$. The multimode HCG allows a unique mechanism to facilitate resonances, which do not fall under either of these two categories. These additional possibilities are a consequence of the matrix $\boldsymbol{\rho}$ being nondiagonal [the only nondiagonal matrix in Eq. (1)]. The nondiagonality of $\boldsymbol{\rho}$ means that the HCG modes couple into each other upon reflections at $z = -t_g$ and $z = 0$. This cross-coupling path does not exist in regular FP cavities, and it is responsible for the strong energy build up within HCG, and for its high Q.

In order to verify that Eq. (1) can predict HCG resonant wavelengths, we plot in Fig. 2(a) a HCG reflectivity spectrum containing five resonances, calculated using RCWA. The five resonances have increasing orders, from first on the right to fifth on the left. Figure 2(b) plots $|\det[\mathbf{I} - (\boldsymbol{\rho}\varphi)^2]|$ as a function of wavelength. It can be seen that the minima of $|\det[\mathbf{I} - (\boldsymbol{\rho}\varphi)^2]|$ indeed match the wavelengths of all five resonances. In addition, the narrowest of the five resonances corresponds to the smallest $|\det[\mathbf{I} - (\boldsymbol{\rho}\varphi)^2]|$, in agreement with Eq. (1).

Equation (1) describes an idealized ("infinite" Q) resonance. Next, we proceed to formulate a general expression for HCG resonances with *finite* quality factors,

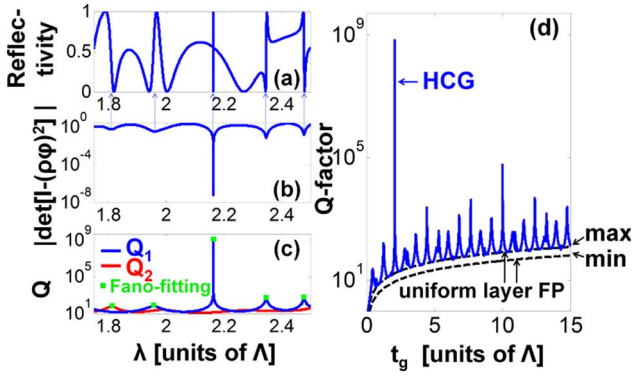

Fig. 2. (Color online) Validation of the HCG resonance condition $\det[\mathbf{I} - (\boldsymbol{\rho}\varphi)^2] = 0$ and of the Q-factor formulation in Eqs. (3) and (4). (a) Surface-normal reflectivity spectra of an HCG-R consisting of five resonances calculated using RCWA [15], (b) determinant versus wavelength, (c) the HCG Q factor obtained from Eqs. (3) and (4) compared with that from Fano fitting. The overall Q factor of the HCG is maximal among Q_1 and Q_2. The Q-factor spikes are shown to precisely predict the wavelengths of the resonances in (a). (d) The dependence of HCG-R Q factor on HCG thickness (blue), as dictated by Eq. (4), compared with a uniform dielectric FP layer (Eq. (2)). The uniform layer Q oscillates (not plotted) between maximum and minimum values (both plotted) as a function of thickness. This variation is very small compared with Q_{HCG}.

whereby the individual supermodes reproduce themselves after each round trip, up to a multiplicative factor, which is not unity. The strategy is simply finding the Q factors of each supermode and arguing that the maximum among them is approximately the Q factor of the entire structure. Let us start with a well-known expression for the Q factor of a regular FP resonator (n_{gr} being the effective group index of the FP cavity):

$$Q = 2\pi n_{\mathrm{gr}} \frac{t}{\lambda} \left| \frac{\rho}{1-\rho^2} \right|. \quad (2)$$

Similarly, each HCG supermode has its own FP Q factor, Q_j, the formulation of which is similar to Eq. (2):

$$Q_j = 2\pi n_{\mathrm{gr}} \frac{t_{\mathrm{g}}}{\lambda} \left| \frac{r_j}{1-r_j^2} \right|, \quad \text{where } r_j = \text{eigenvalues}(\rho\varphi). \quad (3)$$

The supermodes are eigensolutions of HCG, and therefore r_j in Eq. (3) is the jth eigenvalue of the matrix $\rho\varphi$. In the case of a continuous excitation by an incident plane wave, energy will gradually start building up within each supermode. The supermode with the highest Q_j will build up energy faster than the rest, and will eventually dominate. Therefore, we can assign the overall HCG Q factor as the *maximal* among the Q_j in Eq. (3):

$$Q_{\mathrm{HCG}} = \max_j(Q_j) \quad (4)$$

It is easy to prove that the resonance condition in Eq. (1) is equivalent to $Q_{\mathrm{HCG}} \to \infty$ in Eq. (4), since both conditions are only satisfied if one of the eigenvalues r_j equals either $+1$ or -1. The Q factor formalism described in Eqs. (3) and (4) can be verified against a known method for Q-factor extraction by spectral-curve fitting to Fano resonance line shapes [16]. The agreement between the two methods is excellent, as shown in Fig. 2(c), which plots the two largest Q_j's: Q_1 and Q_2. As expected, $Q_{\mathrm{HCG}} = \max(Q_1, Q_2)$ in Fig. 2(c) also exhibits peaks at the exact resonance wavelengths. In addition, the highest Q_{HCG} value indeed corresponds to the sharpest resonance in Fig. 2(a). It is important to emphasize that our Q-factor calculation does not rely on curve fitting. Rather, we calculate the Q factor directly from the HCG geometry using Eqs. (3) and (4). Notably, HCG design can be optimized to reach a Q value as high as 10^9 [Fig. 2(c)].

Figure 2(d) presents Q_{HCG} as a function of HCG thickness. The Q-factor spikes are shown to be nearly periodic with thickness. This periodic pattern attests to the FP nature of HCG resonator and is distinctly different from other structures, such as second-order gratings or photonic crystals. We note that the maximum Q value is not always repeated at larger thicknesses, since the phase matching conditions are not precisely repeated in the multimode case. Also in Fig. 2(d), as a baseline comparison, we show the Q factor of a uniform dielectric layer [Eq. (2)] having the same refractive index as the HCG. In this case, the Q value is oscillating as a function of layer thickness (not shown), while being bound between an upper and a lower limit, both shown by the two dashed black curves in Fig. 2(d). Indeed, the multimode nature of HCG facilitates Q factors orders of magnitude higher than those of a uniform dielectric layer with the same n_r.

The important attributes of HCG that make high-Q resonances possible are: (1) Subwavelength periodicity ($\Lambda < \lambda$), which eliminates nonzero diffraction orders (in the surface-normal configuration); (2) The high refractive index contrast between HCG and the outside planes enhances the coupling between the modes upon reflection at $z = -t_g$ and $z = 0$; (3) The high refractive-index contrast between the grating bars and air gaps typically limits the number of propagating modes over a broad wavelength range to two. Finally, we note that it is particularly simple to design HCG-R for a wide range of wavelengths since dimensions are scalable with wavelength.

In conclusion, in this Letter we have presented a simple explanation for the multimode FP mechanism of resonant HCGs. Our theory facilitates a new simple formalism for the Q factor of HCG. We present a design with a Q value as high as 10^9. Advantages of HCG over other FP resonators were also discussed.

We gratefully acknowledge the support of United States Department of Defense National Security Science and Engineering Faculty Fellowship N00244-09-1-0013 and National Science Foundation (NSF) grants EEC-0812072 and ECCS-1002160, as well as the National Natural Science Foundation of China (NSFC) under grant 61071084, and the State Key Laboratory of Advanced Optical Communication Systems and Networks, China.

References

1. L. Li, J. Mod. Opt. **40**, 553 (1993).
2. C. W. Haggans, L. Li, and R. K. Kostuk, J. Opt. Soc. Am. A **10**, 2217 (1993).
3. E. B. Grann, M. G. Moharam, and D. A. Pommet, J. Opt. Soc. Am. A **11**, 2695 (1994).
4. S. Goeman, S. Boons, B. Dhoedt, K. Vandeputte, K. Caekebeke, P. Van Daele, and R. Baets, IEEE Photonics Technol. Lett. **10**, 1205 (1998).
5. Y. Zhou, M. C. Y. Huang, C. Chase, V. Karagodsky, M. Moewe, B. Pesala, F. G. Sedgwick, and C. J. Chang-Hasnain, IEEE J. Sel. Top. Quantum Electron. **15**, 1485 (2009).
6. C. F. R. Mateus, M. C. Y. Huang, Y. Deng, A. R. Neureuther, and C. J. Chang-Hasnain, IEEE Photonics Technol. Lett. **16**, 518 (2004).
7. M. C. Y. Huang, Y. Zhou, and C. J. Chang-Hasnain, Nat. Photon. **1**, 119 (2007).
8. M. C. Y. Huang, Y. Zhou, and C. J. Chang-Hasnain, Nat. Photon. **2**, 180 (2008).
9. Y. Zhou, M. Moewe, J. Kern, M. C. Y. Huang, and C. J. Chang-Hasnain, Opt. Express **16**, 17282 (2008).
10. P. Lalanne, J. P. Hugonin, and P. Chavel, J. Lightwave Technol. **24**, 2442 (2006).
11. S. Kaushik, J. Opt. Soc. Am. A **14**, 596 (1997).
12. L. C. Botten, N. P. Nicorovici, A. A. Asatryan, R. C. McPhedran, C. M. de Sterke, and P. A. Robinson, J. Opt. Soc. Am. A **17**, 2165 (2000).
13. V. Karagodsky, M. C. Y. Huang, and C. J. Chang-Hasnain, in *Conference on Lasers and Electro-Optics (CLEO)* (Optical Society of America, 2008), paper JTuA128.
14. V. Karagodsky, F. Sedgwick, and C. J. Chang-Hasnain, Opt. Express **18**, 16973 (2010).
15. M. G. Moharam and T. K. Gaylord, J. Opt. Soc. Am. **71**, 811 (1981).
16. S. Fan, W. Suh, and J. D. Joannopoulos, J. Opt. Soc. Am. A **20**, 569 (2003).